System size dependence of elliptic flows in relativistic heavy-ion collisions

Lie-Wen Chen[1,2] and Che Ming Ko[3]

[1]*Institute of Theoretical Physics, Shanghai Jiao Tong University, Shanghai 200240, China*
[2]*Center of Theoretical Nuclear Physics, National Laboratory of Heavy Ion Accelerator, Lanzhou 730000, China*
[3]*Cyclotron Institute and Physics Department, Texas A&M University, College Station, Texas 77843-3366*

(Dated: July 30, 2018)

The elliptic flows in both Cu+Cu and Au+Au collisions at the Relativistic Heavy Ion Collider are studied in a multi-phase transport model. For both collisions at same reduced impact parameter and minimum bias collisions, the elliptic flow of partons in Cu+Cu collisions is about a factor of three smaller than that in Au+Au collisions at same energy. The reduction factor is similar to the ratio of the sizes of the two colliding systems and is also related to the combined effects of initial energy density and spatial elliptic deformation in the two reactions. A similar system size dependence is also seen in the elliptic flow of charged hadrons from minimum bias collisions.

PACS numbers: 25.75.Ld, 24.10.Lx

arXiv:nucl-th/0505044v2 9 Feb 2006

I. INTRODUCTION

There have been extensive studies on the azimuthal anisotropy of hadron momentum distributions in the transverse plane perpendicular to the beam direction, particularly the elliptic flow v_2, in heavy-ion collisions at various energies [1]. The hadron transverse momentum anisotropy is generated by the pressure anisotropy in the initial compressed matter formed in non-central heavy ion collisions [2, 3] and thus depends on the initial geometry and energy density of a collision as well as the properties of produced matter during the early stage of the collision. For heavy-ion collisions at the Relativistic Heavy Ion Collider (RHIC), it has been shown that not only the larger elliptic flow [4, 5, 6, 7, 8, 9] but also the smaller higher-order anisotropic flows [10, 11, 12, 13, 14, 15, 16] are sensitive to the properties of initial dense matter. To study the dependence of the hadron anisotropic flow on the initial geometry and energy density in a heavy ion collision, one can vary the impact parameter of the collision or the atomic number of colliding nuclei. Although there were already extensive studies on the dependence of elliptic flow on the impact parameter of heavy ion collisions, its dependence on the size of colliding nuclei has only been started recently [17].

In the present work, we use a multi-phase transport (AMPT) model, that includes both initial partonic and final hadronic interactions [18, 19], to study the elliptic flow in both Cu+Cu and Au+Au collisions at $\sqrt{s} = 200$ AGeV at RHIC. In particular, we use the version with string melting, i.e., allowing hadrons that are expected to be formed from initial strings to convert to their valence quarks and antiquarks [20, 21, 22], which has been shown to be able to explain the measured p_T dependence of v_2 and v_4 of mid-rapidity charged hadrons with a parton scattering cross section of about 10 mb. We find that the elliptic flow scales approximately with the size of the colliding system and is also proportional to the product of the spatial elliptic deformation and energy density during the initial stage of a collision.

This paper is organized as follows. In Sec. II, the AMPT model is briefly reviewed. Results for the parton elliptic flow and spatial elliptic deformation as well as their system size dependence are shown in Sec. III, while the system size dependence of the elliptic flow of charged hadrons is shown in Sec. IV. Finally, a brief summary is given in Sec. V.

II. THE AMPT MODEL

The AMPT model [18, 19, 23, 24, 25] is a hybrid model that uses minijet partons from hard processes and strings from soft processes in the Heavy Ion Jet Interaction Generator (HIJING) model [26] as the initial conditions for modeling heavy ion collisions at ultra-relativistic energies. Since the initial energy density in Au+Au collisions at RHIC is much larger than the critical energy density at which the hadronic matter to quark-gluon plasma transition would occur [23, 27], we use the version which allows the melting of initial excited strings into partons [20]. In this string melting scenario, hadrons (mostly pions), that would have been produced from string fragmentation, are converted instead to valence quarks and/or antiquarks with current quark masses. Interactions among these partons are described by Zhang's parton cascade (ZPC) model [28]. At present, this model includes only parton-parton elastic scatterings with an in-medium cross section given by:

$$\frac{d\sigma_p}{dt} \approx \frac{9\pi\alpha_s^2}{2}\left(1+\frac{\mu^2}{s}\right)\frac{1}{(t-\mu^2)^2}, \qquad (1)$$

where the strong coupling constant α_s is taken to be 0.47, and s and t are usual Mandelstam variables. The effective screening mass μ depends on the temperature and density of the partonic matter but is taken as a parameter in ZPC for fixing the magnitude and angular distribution of parton scattering cross section. Since there are no inelastic scatterings, only quarks and antiquarks from the melted strings are present in the partonic matter. The transition from the partonic matter to the hadronic matter is achieved using a simple coalescence model, which

combines two nearest quark and antiquark into mesons and three nearest quarks or antiquarks into baryons or anti-baryons that are close to the invariant mass of these partons. The present coalescence model is thus somewhat different from the ones recently used extensively [29, 30, 31, 32] for studying hadron production at intermediate transverse momenta. The final-state hadronic scatterings are then modeled by a relativistic transport (ART) model [33]. Using parton scattering cross sections of 6-10 mb, the AMPT model with string melting is able to reproduce both the centrality and transverse momentum (below 2 GeV/c) dependence of the elliptic flow [20] and pion interferometry [21] measured in Au+Au collisions at $\sqrt{s} = 130$ AGeV at RHIC [34, 35]. It has also been used for studying the kaon interferometry [36] and the elliptic flow of charmed mesons [37] in these collisions. We note that the above cross sections are significantly smaller than that needed to reproduce the parton elliptic flow from the hydrodynamic model [38]. The resulting hadron elliptic flows in the AMPT model with string melting are, however, amplified by modeling hadronization via quark coalescence [32], leading to a satisfactory reproduction of experimental data.

III. ELLIPTIC FLOW AND SPATIAL ANISOTROPY OF PARTONS

The anisotropic flows v_n of particles are the Fourier coefficients in the decomposition of their transverse momentum spectra in the azimuthal angle ϕ with respect to the reaction plane [39], i.e.,

$$E\frac{d^3N}{dp^3} = \frac{1}{2\pi}\frac{dN}{p_T dp_T dy}[1 + \sum_{n=1}^{\infty} 2v_n(p_T, y)\cos(n\phi)] \quad (2)$$

Because of the symmetry $\phi \leftrightarrow -\phi$ in collision geometry, no sine terms appear in above expansion. For particles at midrapidity in collisions with equal mass nuclei, anisotropic flows of odd orders vanish as a result of the additional symmetry $\phi \leftrightarrow \phi + \pi$. Anisotropic flows generally depend on particle transverse momentum and rapidity, and for a given rapidity the anisotropic flows at transverse momentum p_T can be evaluated according to

$$v_n(p_T) = \langle \cos(n\phi) \rangle \,, \quad (3)$$

where $\langle \cdots \rangle$ denotes average over the azimuthal distribution of particles with transverse momentum p_T. The elliptic flow v_2 can further be expressed in terms of single-particle averages:

$$v_2(p_T) = \left\langle \frac{p_x^2 - p_y^2}{p_x^2 + p_y^2} \right\rangle \quad (4)$$

where p_x and p_y are, respectively, projections of the particle momentum in and perpendicular to the reaction plane.

Since the AMPT model also provides information on the spatial anisotropy of colliding matter, which is responsible for generating the momentum anisotropic flows, it is of interest to introduce the spatial anisotropic coefficient s_n by expressions similar to those for the anisotropic flows v_n but in terms of the spatial distributions of particles in the transverse plane. In particular, the spatial elliptic deformation s_2 or eccentricity can be obtained from

$$s_2 = \left\langle \frac{x^2 - y^2}{x^2 + y^2} \right\rangle, \quad (5)$$

where x and y are, respectively, projections of the particle coordinate in and perpendicular to the reaction plane.

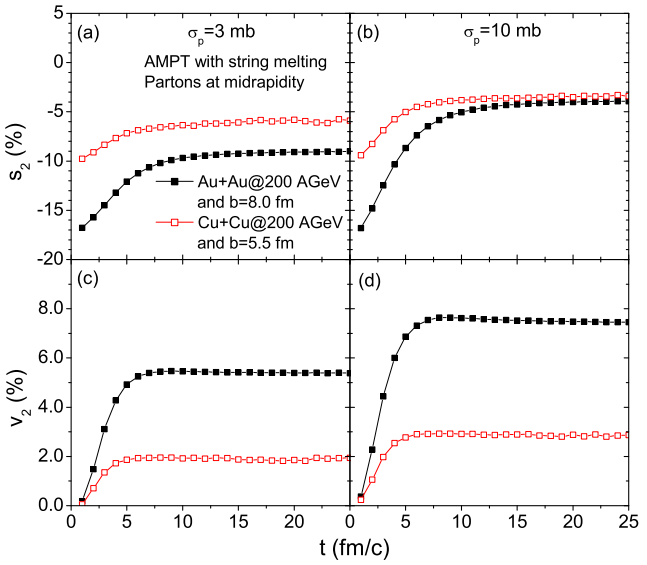

FIG. 1: (Color online) Time evolution of spatial elliptic deformation s_2 and momentum elliptic flow v_2 of partons at midrapidity in Cu+Cu collisions at $b = 5.5$ fm (open squares) and Au + Au collisions at $b = 8$ fm (solid squares) with the same energy per nucleon $\sqrt{s} = 200$ AGeV for parton scattering cross sections $\sigma_p = 3$ mb (left panels) and $\sigma_p = 10$ mb (right panels).

Using the AMPT model in the string melting scenario with parton scattering cross sections $\sigma_p = 3$ and 10 mb, we first study the time evolution of s_2 and v_2 of partons at midrapidity in Cu+Cu collisions at $b = 5.5$ fm and Au+Au collisions at $b = 8$ fm with the same energy per nucleon, i.e., $\sqrt{s} = 200$ AGeV, and the results are shown in Fig. 1. The two impact parameters, which are similar to the average values in minimum bias collisions, correspond to the same reduced impact parameter $b/b_{\rm max}$, where $b_{\rm max}$ is the sum of the radii of colliding nuclei. They would lead to same s_2 if the two nuclei were sharp spheres. Because of diffused surfaces, a much large s_2 is, however, produced in Au+Au collisions than in Cu+Cu collisions as shown in Figs. 1(a) and 1(b). For both collisions, the spatial elliptic deformation s_2 is initially large and decreases with time. It reaches the saturation value

at times which depend on both the size of the reaction system and the parton scattering cross section. Specifically, the s_2 in Cu+Cu collisions has an earlier saturation time, implying that the fireball (or quark gluon plasma) formed in a smaller reaction system has a shorter lifetime. This behavior is understandable since the larger reaction system has a larger initial parton number density in the transverse plane and thus takes longer time to freeze out. The nonzero spatial elliptic deformation s_2 indicates that the parton spatial distribution is non-spherical at freeze out, with the larger parton scattering cross section leading to a smaller spatial anisotropy.

Time evolution of the elliptic flow v_2 of partons is shown in Figs. 1(c) and 1(d) for the two parton scattering cross sections of 3 and 10 mb, respectively. The elliptic flow v_2 is seen to saturate earlier in the collisions, and the saturation time depends on the size of the reaction system, i.e., at about 5 fm/c for Cu+Cu collisions while about 7 fm/c for Au+Au collisions. This is similar for both parton scattering cross sections, except that the larger one leads to a larger elliptic flow. The shorter saturation time of v_2 in lighter reaction system is consistent with the earlier saturation time of s_2 seen in Figs. 1(a) and 1(b) for that system. An interesting result predicted by the AMPT model is that the parton v_2 in Cu+Cu collisions is significantly smaller than that in Au+Au collisions. For instance, the final values of v_2 of partons are about 1.9% and 2.9% , respectively, for $\sigma_p = 3$ mb and 10 mb in Cu+Cu collisions, and they increase to about 5.4% and 7.5% , respectively, for $\sigma_p = 3$ mb and 10 mb in Au+Au collisions. For both cross sections, the strength of parton v_2 is enhanced by a factor of about 3 from Cu+Cu to Au+Au collisions at same reduced impact parameter, and is roughly similar to the ratio of the sizes of Au and Cu nuclei.

The magnitude of elliptic flow is affected not only by the spatial elliptic deformation but also by the energy density during the initial stage of collisions. In Fig. 2, we show the time evolution of the energy densities of midrapidity partons (upper panel) and their ratio (lower panel) in Cu+Cu collisions at $b = 5.5$ fm (dashed line) and Au+Au collisions at $b = 8$ fm (solid line) for parton scattering cross section of 10 mb. As in Ref. [23], the energy density is calculated for partons in the central cell that has a transverse radius of 1 fm and a longitudinal dimension of 5% of the time t with the time coordinate starting when the two nuclei fully overlap in the longitudinal direction. It is seen that the initial energy density in Cu+Cu collisions is about 2/3 of that in Au+Au collisions. Combining this effect with that due to initial spatial elliptic deformation, which has a ratio of about 1/2 for the two colliding systems, gives a reduction factor of about 1/3, which is comparable to the ratio of the sizes of the two colliding systems. The dependence on the system size seen in the parton elliptic flows from the AMPT model is thus related to the combined effects of initial energy density and spatial elliptic deformation.

The same system size dependence is also seen in the

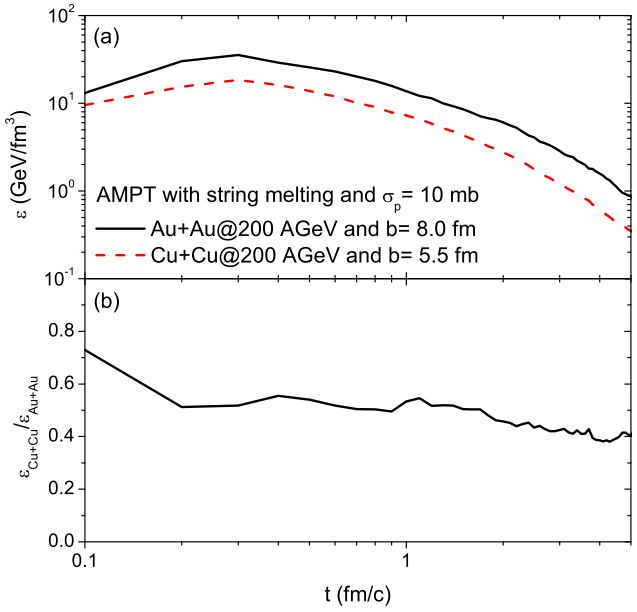

FIG. 2: (Color online) Time evolution of energy densities of midrapidity partons (upper panel) and their ratio (lower panel) in Cu+Cu collisions at $b = 5.5$ fm (dashed line) and Au + Au collisions at $b = 8$ fm (solid line) with the same energy per nucleon $\sqrt{s} = 200$ AGeV for parton scattering cross sections $\sigma_p = 10$ mb.

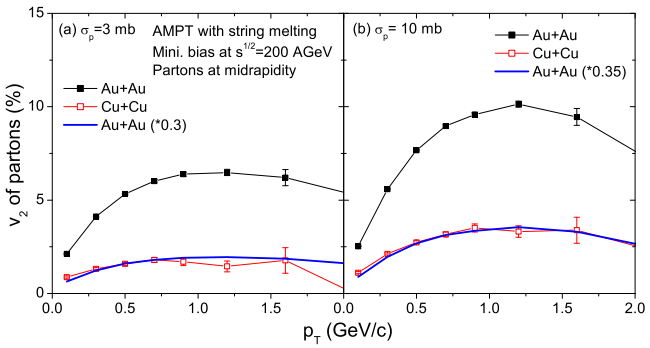

FIG. 3: (Color online) Transverse momentum p_T dependence of v_2 of midrapidity partons from minimum bias events in Au+Au (solid squares) and Cu+Cu (open squares) collisions at $\sqrt{s} = 200$ AGeV for parton scattering cross sections of $\sigma_p = 3$ mb (left panel) and $\sigma_p = 10$ mb (right panel). The solid line is 0.3 (0.35) times v_2 of Au+Au for $\sigma_p = 3$ (10) mb.

parton differential elliptic flow as a function of parton transverse momentum p_T for minimum bias collisions. This is shown in Figs. 3(a) and 3(b) for midrapidity partons from minimum bias events in Au+Au and Cu+Cu collisions at $\sqrt{s} = 200$ AGeV for parton scattering cross sections of 3 mb and 10 mb, respectively. As shown by the solid lines in Figs. 3(a) and 3(b), the parton differential v_2 in Cu+Cu collisions is about 0.3 (0.35) times that in Au+Au collisions for parton scattering cross section of 3 (10) mb.

We note that a detailed comparison between the parton elliptic flows in the two colliding systems further indicates that the parton v_2 in the lighter reaction system is more sensitive to the parton cross sections. For example, the parton v_2 is enhanced by a factor of about 1.53 in Cu+Cu collisions but is enhanced by a factor of about 1.39 in Au+Au collisions, when the parton cross section is increased by a factor of about 3.

IV. SYSTEM SIZE DEPENDENCE OF THE CHARGED HADRON ELLIPTIC FLOW

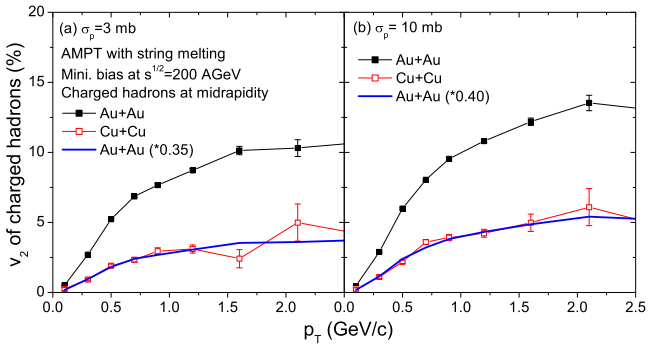

FIG. 4: (Color online) Same as Fig. 3 but for charged hadrons. The solid line is 0.35 (0.4) times v_2 of Au+Au for $\sigma_p = 3$ (10) mb.

The anisotropic flows of partons are transferred to those of hadrons when the latter are formed from the coalescence of quarks and/or antiquarks. Although scatterings among hadrons are included in the AMPT model, they do not affect much the hadron anisotropy flows as a result of the small spatial anisotropy and pressure in the hadronic matter [20]. In Fig. 4, we show the final v_2 of charged hadrons in the pseudorapidity range $|\eta| < 1.2$ in minimum bias Au+Au and Cu+Cu collisions at $\sqrt{s} = 200$ AGeV as functions of the transverse momentum p_T for parton scattering cross sections $\sigma_p = 3$ and 10 mb. It is seen that the charged hadron v_2 in the lighter reaction system Cu+Cu is significantly smaller than that in the heavier reaction system Au+Au. As shown by the solid lines in Figs. 4(a) and 4(b), the charged hadron v_2 in Cu+Cu collisions is about 0.35 (0.4) times that in Au+Au collisions for parton scattering cross section of 3 (10) mb. The elliptic flow of charged hadrons thus shows a similar dependence on the size of the colliding system as that of partons.

A similar dependence on the size of collision system is also seen in the transverse momentum distribution of charged hadrons as shown in Fig. 5. For charged hadrons in the pseudorapidity range $|\eta| < 1.2$ in minimum bias Au+Au and Cu+Cu collisions at $\sqrt{s} = 200$ AGeV for parton scattering cross sections $\sigma_p = 3$ and 10 mb, the transverse momentum spectrum of charged

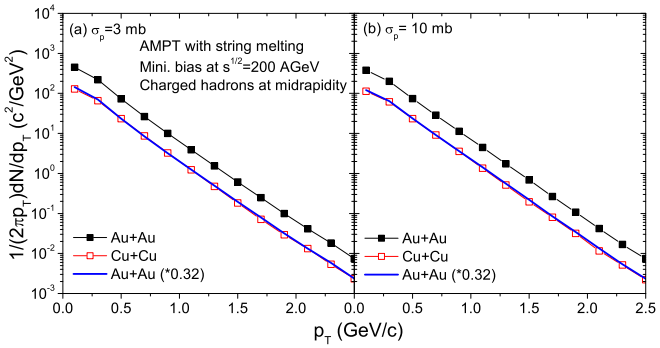

FIG. 5: (Color online) Transverse momentum distribution of charged hadrons in the pseudorapidity range $|\eta| < 1.2$ from minimum bias events in Au+Au (solid squares) and Cu+Cu (open squares) collisions at $\sqrt{s} = 200$ AGeV for parton scattering cross sections of $\sigma_p = 3$ mb (left panel) and $\sigma_p = 10$ mb (right panel). Solid lines are the results from Au+Au collisions that are scaled by 0.32.

hadrons in Cu+Cu collisions is again about 0.32 times that in Au+Au collisions as shown by the solid lines in Figs. 5(a) and 5(b). This implies that the total transverse energy $\langle m_T \rangle$ of hadrons at midrapidity follows the same dependence on the system size. Since the initial energy density in heavy ion collisions can be estimated via $\varepsilon \sim \langle m_T \rangle / (\tau_0 \pi R^2)$ [40], where τ_0 is the formation or thermalization time and R is the radius of the colliding nuclei, the ratio of its values in Cu+Cu and Au+Au collisions is thus

$$\frac{\varepsilon_{\rm Cu+Cu}}{\varepsilon_{\rm Au+Au}} = \frac{\langle m_T \rangle_{\rm Cu+Cu}}{\langle m_T \rangle_{\rm Au+Au}} \cdot \frac{R^2_{\rm Au}}{R^2_{\rm Cu}} \sim 0.68. \qquad (6)$$

This estimated value is consistent with that from the AMPT model shown in Fig. 2.

V. SUMMARY

Using the AMPT model with string melting, we have studied elliptic flows in Cu+Cu and Au+Au collisions at RHIC. We find that for both collisions at same reduced impact parameter and minimum bias collisions, the elliptic flow of partons in the lighter Cu+Cu collisions is about a factor of 3 smaller than that in the heavier Au+Au collisions at same energy, similar to the ratio of the system sizes. By examining the energy density and spatial elliptic deformation during the initial stage of a collision, we further find that their combined effect is similar to the size effect seen in the elliptic flows in the two colliding systems. A similar ratio is predicted for the elliptic flows of charged hadrons in minimum bias collisions of the two systems. Recent preliminary experimental results from the PHOBOS collaboration [17] have shown that if the charge hadron elliptic flow is scaled by the initial eccentricity or spatial elliptic deformation of participant nucleons, its magnitude becomes qualitatively

similar in both Cu+Cu and Au+Au collisions. How our results are related to this observation is of great interest and will be addressed in a subsequent study.

Acknowledgments

This work was supported in part by the National Natural Science Foundation of China under Grant Nos. 10105008 and 10575071 (LWC) as well as by the US National Science Foundation under Grant Nos. PHY-0098805 and PHY-0457265 and the Welch Foundation under Grant No. A-1358 (CMK).

[1] W. Reisdorf and H.G. Ritter, Ann. Rev. Nucl. Part. Sci. **47**, 663 (1997).
[2] J. Barrette *et al.*, E877 Collaboration, Phys. Rev. Lett. **73**, 2532 (1994).
[3] H. Appelshauser *et al.*, NA49 Collaboration, Phys. Rev. Lett. **80**, 4136 (1998).
[4] J.Y. Ollitrault, Phys. Rev. D **46**, 229 (1992).
[5] H. Sorge, Phys. Lett. **B402**, 251 (1997); Phys. Rev. Lett. **78**, 2309 (1997); Phys. Rev. Lett. **82**, 2048 (1999).
[6] P. Danielewicz, R.A. Lacey, P.B. Gossiaux, C. Pinkenburg, P. Chung, J.M. Alexander and R.L. McGrath, Phys. Rev. Lett. **81**, 2438 (1998).
[7] B. Zhang, M. Gyulassy and C.M. Ko, Phys. Lett. **B455**, 45 (1999)
[8] Y. Zheng, C.M. Ko, B.A. Li and B. Zhang, Phys. Rev. Lett. **83**, 2534 (1999).
[9] S.A. Voloshin, Nucl. Phys. **A715**, 379c (2003).
[10] P.F. Kolb, J. Sollfrank, and U. Heinz, Phys. Lett. **B459**, 667 (1999)
[11] D. Teaney and E.V. Shuryak, Phys. Rev. Lett. **83**, 4951 (1999);
[12] P.F. Kolb, J. Sollfrank, and U. Heinz, Phys. Rev. C **62**, 054909 (2000).
[13] P.F. Kolb, Phys. Rev. C **68**, 031902 (R) (2003).
[14] J. Adams *et al.*, STAR Collaboration, Phys. Rev. Lett. **92**, 062301 (2004) .
[15] L.W. Chen, C.M. Ko, and Z.W. Lin, Phys. Rev. C **69**, 031901 (R) (2004).
[16] P. Kolb, L.W. Chen, V. Greco, and C.M. Ko, Rev. C **69**, 051901 (R) (2004).
[17] S. Manly (for the PHOBOS Collaboration), nucl-exp/0510031.
[18] B. Zhang, C.M. Ko, B.A. Li and Z.W. Lin, Phys. Rev. C **61**, 067901 (2000).
[19] Z.W. Lin, S. Pal, C.M. Ko, B.A. Li, and B. Zhang, Phys. Rev. C **64**, 011902 (2001); Nucl. Phys. **A698**, 375 (2002).
[20] Z.W. Lin and C.M. Ko, Phys. Rev. C **65**, 034904 (2002).
[21] Z.W. Lin, C.M. Ko and S. Pal, Phys. Rev. Lett. **89**, 152301 (2002).
[22] C.M. Ko, Z.W. Lin, and S. Pal, Heavy Ion Phys. **17**, 219 (2003).
[23] B. Zhang, C.M. Ko, B.A. Li, Z.W. Lin, and B.H. Sa, Phys. Rev. C **62**, 054905 (2000); B. Zhang, C.M. Ko, B.A. Li, Z.W. Lin, and S. Pal, *ibid.* **65**, 054909 (2002).
[24] S. Pal. C.M. Ko, and Z.W. Lin, Nucl. Phys. **A730**, 143 (2004).
[25] Z.W. Lin, C.M. Ko, B.A. Li, B. Zhang, and S. Pal, Phys. Rev. C **72**, 064901 (2005).
[26] X.N. Wang and M. Gyulassy, Phys. Rev. D **44**, 3501 (1991).
[27] D. Kharzeev and M. Nardi, Phys. Lett. **B507**, 121 (2001).
[28] B. Zhang, Comput. Phys. Commun. **109**, 193 (1998).
[29] V. Greco, C.M. Ko, and P. Lévai, Phys. Rev. Lett. **90**, 202302 (2003); Phys. Rev. C **68**, 034904 (2003).
[30] R.C. Hwa and C.B. Yang, Phys. Rev. C **67**, 034902 (2003); 064902 (2003).
[31] R.J. Fries, B. Müller, C. Nonaka, and S.A. Bass, Phys. Rev. Lett. **90**, 202303 (2003); Phys. Rev. C **68**, 044902 (2003).
[32] D. Molnar and S.A. Voloshin, Phys. Rev. Lett. **91**, 092301 (2003).
[33] B.A. Li and C.M. Ko, Phys. Rev. C **52**, 2037 (1995); B.A. Li, A.T. Sustich, B. Zhang, and C.M. Ko, Int. Jour. Phys. E **10**, 267 (2001).
[34] K.H. Ackermann *et al.*, STAR Collaboration, Phys. Rev. Lett. **86**, 402 (2001).
[35] C. Adler et al., STAR Collaboration, Phys. Rev. Lett. **87**, 082301 (2001).
[36] Z.W. Lin and C.M. Ko, J. Phys. G **30**, S263 (2004).
[37] B. Zhang, L.W. Chen, and C.M. Ko, Phys. Rev. C **72**, 024906 (2005).
[38] D. Molnar and P. Huovinen, Phys. Rev. Lett. **94**, 012302 (2005).
[39] A.M. Poskanzer and S.A. Voloshin, Phys. Rev. C **58**, 1671 (1998).
[40] J.D. Bjorken, Phys. Rev. D **27**, 140 (1983).